Pertanika J. Sci. & Technol. 30 (3): 1755 - 1770 (2022)

PERTANIKA JOURNALS

SCIENCE & TECHNOLOGY

Journal homepage: http://www.pertanika.upm.edu.my/

Modeling and Molecular Dynamics of Aquaporin from an Antarctic *Pseudomonas* sp. Strain AMS3

Muhairil Sulong Tuah[1,2], Wahhida Latip[1,2], Ainur Yasmin Ahmad Ridzwan[1,2], Samyuktha Balakrishnan[1,2], Raja Noor Zaliha Raja Abd. Rahman[1], Noor Dina Muhd Noor[1,2] and Mohd Shukuri Mohamad Ali[1,2]*

[1]*Enzyme and Microbial Technology Research Centre, Faculty of Biotechnology and Biomolecular Sciences, Universiti Putra Malaysia, 43400 UPM, Serdang, Selangor, Malaysia*
[2]*Department of Biochemistry, Faculty of Biotechnology and Biomolecular Sciences, Universiti Putra Malaysia, 43400 UPM, Serdang, Selangor, Malaysia*

ABSTRACT

Aquaporins, also known as water channels, are a large family of transmembrane channel proteins present throughout all life domains and are implicated in human disorders. The psychrophilic aquaporin comes to attention because of its specialty in adaptive ability to keep on functioning to maintain water homeostasis under low temperatures, which have an optimal temperature for growth at about 15ºC or lower. However, studies regarding aquaporin isolated from psychrophilic *Pseudomonas* sp. are still scattered. Recently, the genome sequence of an Antarctic *Pseudomonas* sp. strain AMS3 revealed a gene sequence encoding for a putative aquaporin designated as PAqpZ2_AMS3. In this study, structure analysis and molecular dynamics (MD) simulation of a predicted model of a fully hydrated aquaporin monomer was embedded in a lipid bilayer and was performed at different temperatures for structural flexibility and stability analysis. The MD simulation results revealed that the predicted structure could remain stable and flexible at low to medium temperatures. In addition, the important position of water gating amino acids, Phe36 and Asn180 residues were rearranged in -5ºC MD simulation, leading to changes in the aquaporin water column size. The information obtained from this psychrophilic aquaporin, PAqpZ2_AMS3, provides new insights into the structural

ARTICLE INFO

Article history:
Received: 08 October 2021
Accepted: 16 December 2021
Published: 20 April 2022

DOI: https://doi.org/10.47836/pjst.30.3.01

E-mail addresses:
muhairilst@gmail.com (Muhairil Sulong Tuah)
wahhidalatip@gmail.com (Wahhida Latip)
yasmin97ay@gmail.com (Ainur Yasmin Ahmad Ridzwan)
gs59053@student.upm.edu.my (Samyuktha Balakrishnan)
rnzaliha@upm.edu.my (Raja Noor Zaliha Raja Abd. Rahman)
dina@upm.edu.my (Noor Dina Muhd Noor)
mshukuri@upm.edu.my (Mohd Shukuri Mohamad Ali)
* Corresponding author

ISSN: 0128-7680
e-ISSN: 2231-8526

adaptation of this protein at low temperatures and could be a useful tool for low-temperature industrial applications and molecular engineering purposes in the future.

Keywords: Antarctica, aquaporin, homology modeling, molecular dynamics, *Pseudomonas* sp. AMS3, water gating

INTRODUCTION

Aquaporin is known as one of the integral membrane channel proteins which belong to the major intrinsic protein (MIP) family responsible for maintaining water homeostasis in a cell by facilitating the water movement across the cell membranes. These channels are highly selective with passively transporting water and other small polar molecules. Previously reported research on aquaporin revealed that the protein structures consist of the conserved structural fold with six transmembrane helices and five loops with a single narrow pore at the center of the structure **(**Gomes et al., 2009). Aquaporin signature Asparagine-Proline-Alanine (NPA) motif constitutes the center of the channel. Other than that, facing the extracellular side of the protein also contain a conserved constriction region of aromatic/Arginine (ar/R) motif that acts as the selectivity filter in facilitating the water or other small polar molecules movement across the membrane (Aponte- Santamaría et al., 2017; Brown, 2017; Lind et al., 2017; Araya-Secchi et al., 2011).

Another member of the MIP family, the aquaglyceroporin (Glp), is known to have a less pronounced periplasmic protrusion, where it allows the permeation of glycerol alongside the water molecules. This Glp possesses the same NPA motifs as aquaporin, which serve as the crucial structural domain that plays a role in permeation selectivity. The ar/R constriction site impairs the entrance of high molecular weight substrates, which is around 3.4 Å, compared to only 2.8 Å for the aquaporin. This region is composed of a different set of amino acids that will allow the passage of wider compounds such as glycerol. For example, the smaller Glycine residue in aquaglyceroporin could provide a hydrophobic corner that interacts with bigger molecules (Hub et al., 2009; Gomes et al., 2009).

Useful discovery of the aquaporin gating provided by high-resolution aquaporin structures and molecular dynamics (MD) simulations categorized the mechanisms as capping and pinching (Hedfalk et al., 2006). The regulation of water movement across the aquaporin channel is by either gating, which controls the water flow rate through the channel, or by targeting the aquaporin to different membranes, known as trafficking (Sachdeva & Singh, 2014). As studied by Woo et al. (2008), the phosphorylation of Serine or Threonine residues may or may not involve the membrane trafficking mechanism of aquaporin. Besides that, Németh-Cahalan and Hall (2000) mentioned that changes in pH provide a feedback signal which regulates the aquaporin water permeability. Changes in divalent cation concentrations are also common signals utilized as gating for the aquaporin channel (Kourghi et al., 2017). In addition, Sachdeva and Singh (2014) stated that the

involvement of a single or few residues movement that results in small conformational changes of the aquaporin leads to water flow blockage through the channel.

In a low-temperature environment, unfavorable cell water loss is a critical adaptive mechanism for an organism to prevent osmotic shock and injury or cell death from internal ice formation (Goto et al., 2015). The psychrophilic aquaporin comes to attention because of its specialty in adaptive ability to keep on functioning to maintain water homeostasis under the temperatures. So far, functional studies of aquaporin that have been done were for mesophilic organisms (Aponte-Santamaría et al., 2017; Sachdeva & Singh, 2014), thermophilic microorganisms (Araya-Secchin et al., 2011; Mathai et al., 2009; Kozono et al., 2003) and psychrophilic insect (Goto et al., 2015; Cohen, 2012). The recent completion of a genome project of polar bacteria isolated from Antarctic soil revealed the presence of aquaporin in *Pseudomonas* sp. Strain AMS3. With this available genomic dataset, the structure of the bacterial aquaporin was predicted and studied using appropriate computer-aided software, and (MD) simulation was used to study its functional adaptation at various low temperatures. Molecular dynamics have been considered a powerful and useful computational tool as it provides more information and understanding of the molecular mechanism at a molecular scale, especially for the study of aquaporin (Hospital et al., 2015; Hub et al., 2009).

Antarctic habitat proved that staying dehydrated is important to survive under low temperatures and desiccation stress, where this important water metabolism control is ruled by aquaporin (Goto et al., 2015). Aponte-Santamaría et al. (2017) stated that aquaporin gating might influence the rapid change in water transport activity, and various external stimuli may trigger this gating. Tyr31 acts as aquaporin gating residue from the Aqy1 genome, the water transporting aquaporin in *Pichia pastoris* results in the microorganism death after undergoing multiple freeze/thaw cycles. When comparing the position of the residue at room temperature and low temperature, the simulation data of Aqy1 in a freezing environment shows a movement of about 0.5Å towards the cytoplasm. It leads to changes in the size of the pore water column that results in blockage of the channel. Thus, it can be concluded that temperature changes cause this change.

This paper reported for the first time the homology modeling and molecular dynamics studies of aquaporin from an Antarctic *Pseudomonas* sp. AMS3, to the best of the authors' knowledge. The three-dimensional structures of the putative aquaporin were predicted and evaluated using appropriate software. The structural properties of the putative aquaporin at various temperatures were studied using molecular dynamics (MD) simulations and were discussed. More research is needed to understand the psychrophilic aquaporin, which could contribute to biomimetic membrane approaches for water filtration technologies. As a result, industrial wastewater treatment will particularly benefit the food and beverage and pharmaceutical industries.

METHODOLOGY

Sequence Alignment of PAqpZ2_AMS3

Recently, the genome sequence project of an Antarctic isolate, *Pseudomonas* sp. strain AMS3 was completed by Codon Genomics Sdn Bhd. Genome mining for aquaporin revealed the gene encoding for the putative aquaporin. The identified amino acid sequence designated as PAqpZ2_AMS3, consisting of 231 amino acid residues respectively, was used for the sequence analysis and modeling. First, the aquaporin amino acid sequence was named based on its scaffold position identified in the structural annotation. Then, the homologous sequence was identified using the BLAST program (Donkor et al., 2014; Altschul et al., 1990). Next, multiple sequence alignment was carried out using ClustalW open software with the amino acid sequence from the nearest hit in BLAST result and aquaporin crystal structure sequence isolated from *E. coli*.

Homology Modeling and Validation

SWISS-MODEL homology modeling (Bienert et al., 2017) open software was used to identify the most suitable template and build the 3D model for PAqpZ2_AMS3. The template used for the modeling was the 2.5 Å crystal structure of Aquaporin Z obtained from *Escherichia coli* (strain K12) (PDB ID: 1RC2) (Savage et al., 2003) based on the highest percentage of similarity in BLAST. The structure validation was assessed with ERRAT to compare the six types of non-bonded atom-atom interactions (CC, CN, CO, NN, NO, and OO) of the modeled structures with a reliable high-resolution structure database (Kleywegt, 2000; Colovos & Yeates, 1993) and Ramachandran plot to evaluate the structures' geometrical aspects (Mannige et al., 2016; Zhou et al., 2011).

Software

The molecular dynamics (MD) simulations were performed using the Yet Another Scientific Reality Application (YASARA) software program version 10.2.1 on the predicted aquaporin model structure (Krieger & Vriend, 2014). In addition, AMBER03 (Assisted Model Building with Energy Refinement) force field package was used to conduct the simulation as it includes a set of advanced molecular mechanical force fields for a suite of molecular simulation programs (Salomon-Ferrer et al., 2013).

Molecular Dynamics (MD) Simulations at Various Temperature

This study seeks to investigate membrane simulation of the predicted models at the temperatures of -5°C, 0°C, 5°C, 15°C, and 37°C. A 10 ns of membrane simulation was performed with the first nanosecond considered an equilibration period, and the last 10

ns were used for analysis. AMBER03 force field parameter implemented in the YASARA software was employed for the system's proteins, phospholipids, and water molecules.

The initial model was oriented and embedded in the membrane by the software after it scanned for the secondary structure elements with hydrophobic surface residues of the protein. The simulated system consisted of the PAqpZ2_AMS3 monomer embedded in a fully solvated lipid bilayer of approximately 167 phosphatidylethanolamines (PEA). In addition, the bilayer was fully solvated with 8643 (PAqpZ2_AMS3) clear water and NaCl molecules. Subsequently, the initial model was energy-minimized in each simulation. Before the real simulation, 250 ps of restrained equilibration simulation was run to ensure the adaptability of the new embedded protein in the membrane.

Simulation Analysis

PAqpZ2_AMS3 monomer was studied using 400 saved steps for each simulation. The data obtained were analyzed using YASARA tools as the analysis provides a better understanding of the dynamic properties of the protein-embedded membrane in water at different temperatures. Furthermore, the root mean square deviations of Cα (Cα-RMSD) were computed to measure the magnitude of each amino acid's conformational change to evaluate each residue's stability and flexibility at different temperatures. Besides, the fluctuation of Cα (Cα-RMSF) was also computed for each aquaporin monomer per residue to study the trajectories' flexibilities.

Further analysis was performed by calculating and estimating the pore radius for the final simulated aquaporin model structures at different temperatures. The channel geometry was monitored by computing the pore radius profile in the z-direction that fits in the channel space without overlapping the van der Waals surfaces of the surrounding residues using the HOLE 2.0 program software (Brezovsky et al., 2013). In addition, a superimposition image of the aquaporin was generated with UCSF Chimera software to compare distinct residues that were influenced by different temperatures during the simulation period.

RESULTS AND DISCUSSION

Sequence and Structure Comparisons

Sequence Analysis. Gene sequence encoding for a putative aquaporin was identified from an Antarctic *Pseudomonas* sp. strain AMS3 and designated PAqpZ2_AMS3. The sequence analysis using BLAST (Donkor et al., 2014) showed that the protein sequence represented members of classical water aquaporin within the classical aquaporin subfamily named AqpZ. All aquaporin consists of an NPA motif which is similar to PAqpZ2_AMS3. Two sets of NPA motifs were identified in sequence alignment Figure 1 box in red color. This agreement with aquaporin isolated from *Methanothermobacter marburgensis* consists of

two NPA motifs in the protein sequence (Colovos & Yeates, 1993). Moreover, the NPA motif was reported to have a significant role in proton exclusion during water movement through the aquaporin pore (Finn & Cerda, 2015).

To distinguish between AqpZ and Glps is the conserved amino acid residue, the ar/R region (Tong et al., 2019), which functions as a selective filter. The AqpZ ar/R region is F(H/I)XR which are F43, H172, R187, and carbonyl of T181 in PAqpZ2_AMS3 protein marked with a blue arrow in Figure 1. The combination of these four residue side chains located at the construction site of the aquaporin determines the pore size of the water channel protein and the protein structural organization (Lind et al., 2017). Moreover, the BLAST result showed that sequence similarity between identified aquaporin scores is 63% from sequence identity, *E. coli* AqpZ (PDB ID: 1RC2). The percentage similarity of 63% was the highest score in the sequence database and is known to be sufficient to compare and confirm the identified aquaporin, PAqpZ2_AMS3. It is supported by the similarity with the sequences having the same important motifs as highlighted in Figure 1.

Modeling and Validation of Aquaporin Structure. The homology modeling pipeline aims for the modeling template which optimally covers the target sequence length to maximize the expected quality of the models and the coverage of the target (Mathai et al., 2009). This study modeled the predicted structure using a crystal structure of aquaporin from *Escherichia coli* strain K12 (PDB ID: 1RC2) (Savage et al., 2003). It is due to its highest quality selected by the SWISS-MODEL homology modeling server for model building with

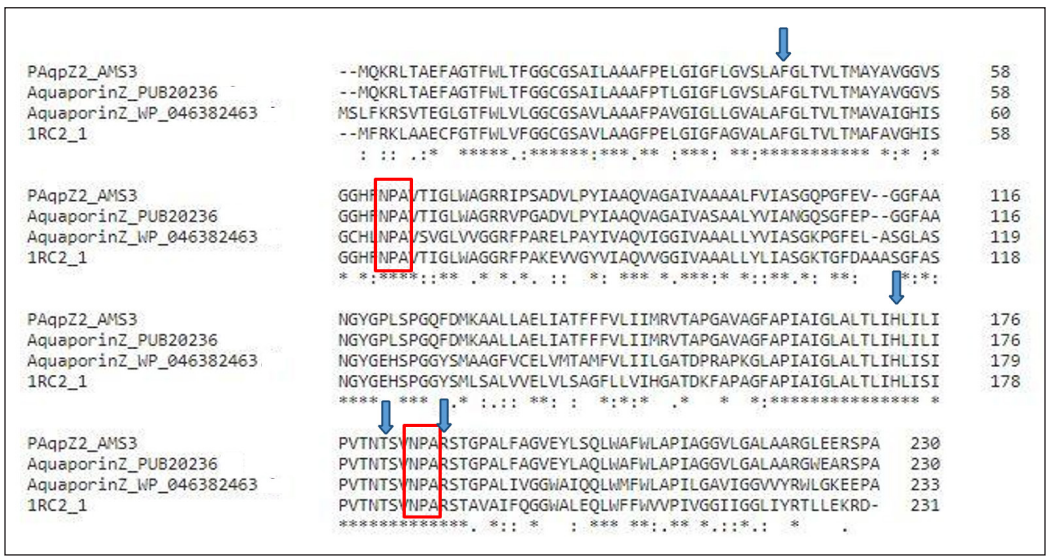

Figure 1. The sequence alignment of both identified putative aquaporins from Antarctic *Pseudomonas sp*. AMS3 (PAqpZ2_AMS3); *Pseudomonas sp.* GV105 (PUB20236); *Pseudomonas sp.* (WP_046382463) and *E. coli* AqpZ (1RC2). The conserved NPA motif regions (red box) and the selectivity filter or ar/R constriction region (blue arrow) are indicated.

a score of 65% for sequence identity of PAqpZ2_AMS3, respectively.

The aquaporin model quality was verified using the Ramachandran plot and ERRAT before MD simulation. It is because to see the reliability of the predicted structure. Figure 2 and Table 1 indicate the score obtained for structure validation of the aquaporin model structure using stated programs. Ramachandran plot provides a way to indicate the quality of a three-dimensional protein structure as it can display the distribution of torsion angles known as Phi (ϕ) and Psi (ψ) angles in a protein structure and an overview of excluded regions that shows which rotation of the polypeptide is not allowed due to the steric hindrance (Zhou et al., 2011). The predicted structure showed a high-quality model where the score is up to 97.8% (PAqpZ2_AMS3) for localization validation. The residues within the select region were 92.1%, and those in the additional allowed region were 5.7%. In addition, amino acids such as Gln 126, Thr 181, and Val 197 contribute to the outer region.

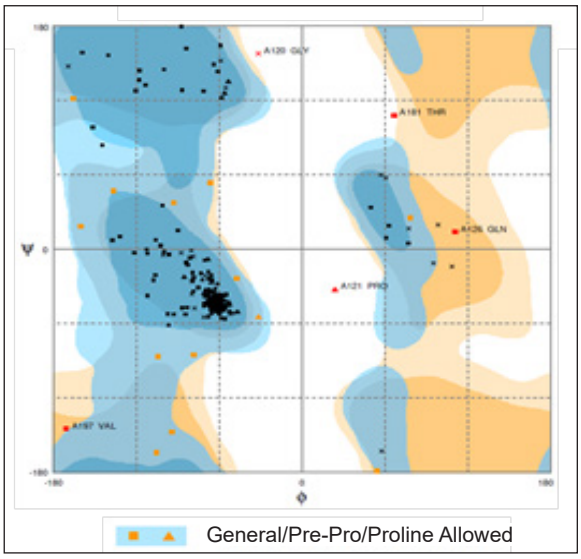

(a)

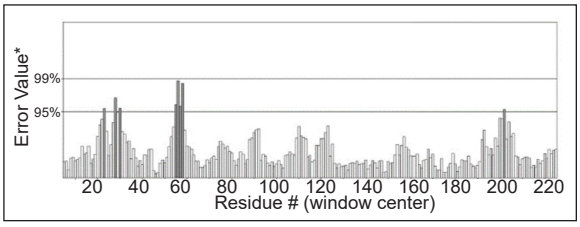

(b)

Figure 2. Validation of the predicted aquaporin three-dimensional model: (a) Ramachandran plot; and (b) ERRAT. The predicted 3D aquaporin model structure was of good quality because most residues can be seen clustered at the most favored region and were within an acceptable overall structure quality factor for the lower resolution of structures.

Table 1
Details of Ramachandran plot and ERRAT results

Ramachandran plot statistics	**PAqpZ2_AMS3**
Residues in favored region	92.1%
Residues in the allowed region	5.7%
Residues in outlier region	2.2%
ERRAT Overall quality factors	96.4%

Low-resolution structures generally produce an average overall quality factor of around 91%, and the calculated error value falls below 95% of the rejection limit (Colovos & Yeates, 1993). PAqpZ2_AMS3 structure showed above 95% as in Table 1 for ERRAT validation. The ERRAT program assesses the predicted protein structure by comparing the six types of non-bonded atom-atom interactions (CC, CN, CO, NN, NO, and OO) of

the modeled structures with a reliable high-resolution structure available in the database (Kleywegt, 2000). In conclusion, the predicted structure is a high-quality structure used for MD simulation.

Structure Analysis. The model structure built was compared and superposed with its template, the crystal structure of AqpZ (PDB ID: 1RC2), using UCSF Chimera (Figure 3). The predicted three-dimensional aquaporins show similar structural properties as Lind et al. (2017) reported research on aquaporin where the protein structures consist of the conserved structural fold with six transmembrane helices and five loops with a single narrow pore at the center of the structure. The structure that showed differences between AqpZ and PAqpZ2_AMS3 is zoomed in the box. Moreover, the center of the channel consists of the aquaporin signature Asparagine-Proline-Alanine (NPA) motif [Figure 4 (b)]. Besides, the aquaporin's conserved constriction region of aromatic/Arginine (ar/R) motif positioned which are Phe; His; Thr, and Arg at the extracellular side of the protein that acts as the selective filter [Figure 4 (a)] (Brown 2017; Araya-Secchin et al., 2011; Goto et al., 2015).

Based on the superimposition of the aquaporin in Figure 3, the overall Root Mean Square Deviation (RMSD) of the protein alpha carbon was calculated using the UCSF Chimera software. The calculated Cα-RMSD between the predicted model with its model template is 0.27Å respectively. Comparing the conserved constriction region and the NPA motif of the aquaporins (Figure 4), calculated Cα-RMSD is not showing an obvious difference, with an average only of 0.06Å. The highest Cα-RMSD can be found at the residues located at the top of the aquaporin structure, as indicated in the box in Figure 3. The

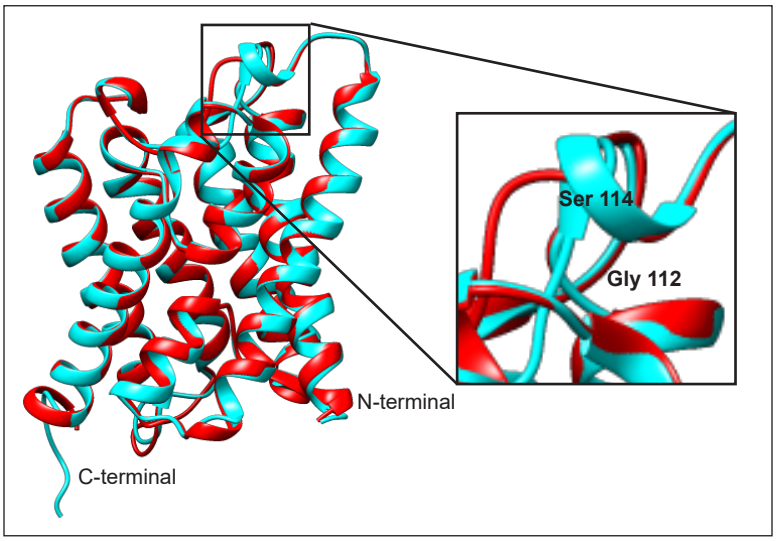

Figure 3. The superimposition of the aquaporin model and its template 3D structure. The aquaporins are red for PAqpZ2_AMS3 and cyan for template AqpZ (PDB ID: 1RC2). The zoomed figure shows the highest Cα-RMSD residues calculated by UCSF Chimera between the aquaporin structures.

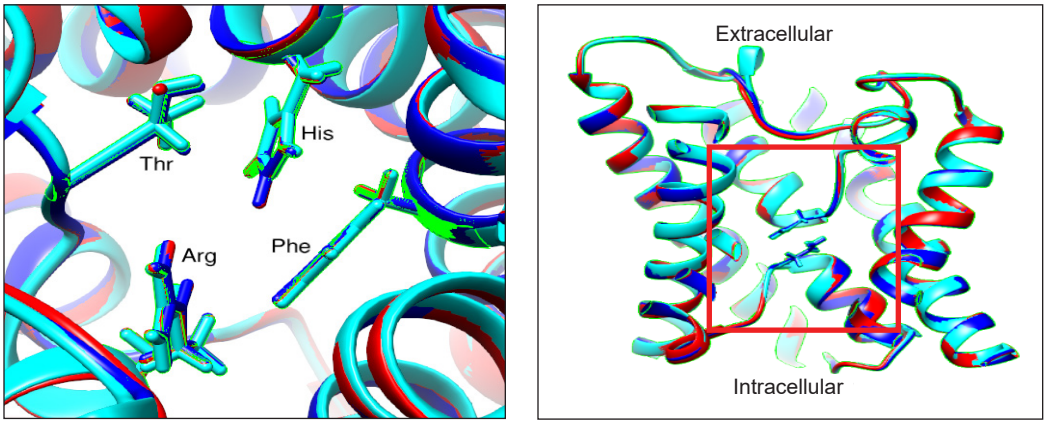

(a) (b)

Figure 4. Zoom-in of the superimposition of the aquaporin model and its template 3D structure. The aquaporins are indicated as red for PAqpZ2_AMS3 and cyan for template AqpZ. (a) ar/R region details of superposed models. (b) NPA motif region details are indicated in the red box (Asn63, Pro64, Ala65, Asn184, Pro185, Ala186).

highest difference was between the Gly112 of PAqpZ2_AMS3 and Ser114 of AqpZ with 3.34Å. It indicates that the modeling of putative aquaporin obtained from the *Pseudomonas* sp. AMS3 shows a slight difference in structural properties with its template, which is a solved aquaporin crystal structure, AqpZ.

Other than that, De Maayer et al. (2014) mentioned that a low number of hydrogen bonds could be found in psychrophilic protein as it is important for the protein's conformational flexibility under a cold environment. In agreement with these statements, the hydrogen bond calculated using UCSF Chimera in each predicted aquaporin model and its template, AqpZ, shows a difference of up to hundreds of hydrogen bonds in number. For example, the hydrogen bond calculated in PAqpZ2_AMS3 was 203, respectively. However, compared to the template used, which originates from a mesophilic microorganism (*E. coli*), 307 hydrogen bonds were calculated in the AqpZ.

Molecular Dynamics (MD) Simulation

MD simulation was performed in this study to discover the aquaporin's structural, flexibility, and dynamics changes identified in different temperatures. Theoretically, the density of water varies with temperature as it depends on this parameter (Cho et al., 2002). The monomer of predicted aquaporin was used for the MD simulation. Schmidt and Sturgis (2017) revealed that the tetrameric nature of aquaporins is important to remain stable while integrated within the bilayer membrane and perform its function. However, they added that the monomeric structure of aquaporin in some family members does not affect the protein's role in facilitating the water movement across the membrane. In concurrence with previous studies, the aquaporin monomers used in this study also appear to integrate into

the membrane normally since the secondary structure of the aquaporin monomer contains a lot of hydrophobic residues that can be a part of the transmembrane region of the protein.

The predicted aquaporins were also suggested to be a psychrophilic protein. Increasing the temperature to 37°C may raise the kinetic energy and result in the conformational changes of the psychrophilic aquaporin due to the intermolecular forces disruption, leading to dysfunction of the protein. The coordinates of the last frame from the conformational sampling were saved to analyze its water column structure.

Molecular Dynamics (MD) Simulation Analysis

By calculating the Root Mean Square Deviation values of the C-alpha (Cα-RMSD) relative to the coordinates of the energy-minimized initial structures, the overall changes in the model atomic coordinates were monitored during MD simulations as a function of time. For example, the convergence of RMSD values from the minimized predicted aquaporin structure during the simulation at -5ºC, 0ºC, 5ºC, 15ºC, and 37ºC after a period are shown in Figure 5.

At the first nanosecond of PAqpZ2_AMS3 at -5ºC, the RMSD value fluctuates almost to a value of 4.0 Å. This obvious fluctuation by the protein can be considered acceptable. In MD simulation, there is an equilibration phase where the membrane is artificially stabilized to adapt to the newly embedded aquaporin and the right density without being damaged. Overall, the predicted aquaporin model can be deduced as stable simulated in different temperatures throughout the simulation. The protein can maintain its structural stability after the first nanosecond of the simulation. Besides, the protein structure did not diverge more than 3.0 Å towards the end of the simulation at 10 ns, implying that the protein had reached its structural equilibrium with the membrane lipids. In addition, the aquaporin

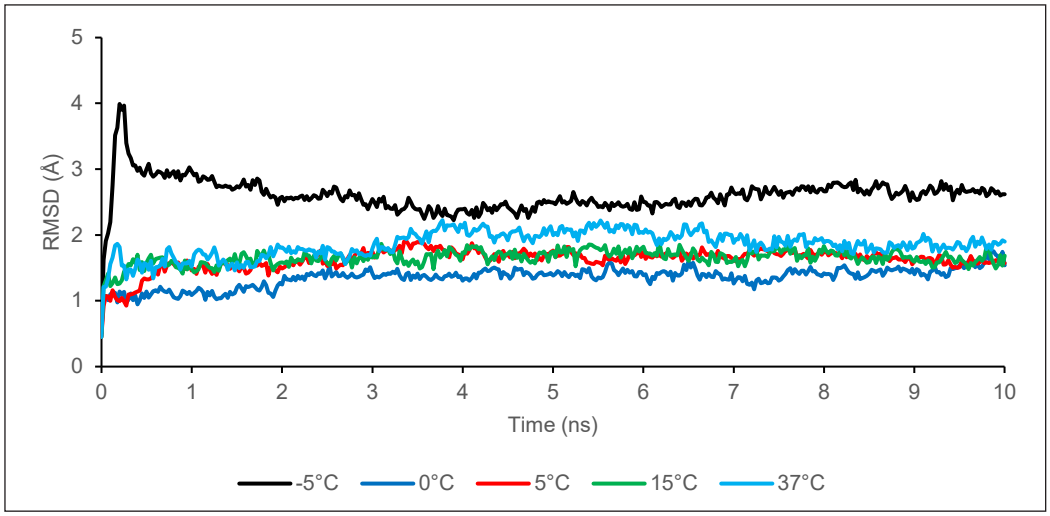

Figure 5. Root Mean Square Deviation (RMSD) of the Carbon alpha as functions of time for PAqpZ2_AMS3

model also showed a stable conformation when simulated at 37ºC as structural changes should be seen as the temperature rises.

Figure 6 depicts the Root Mean Square Fluctuation (RMSF) per residue of the predicted aquaporin model simulated at -5ºC to 37ºC with the initial model secondary structure displayed at the top. The fluctuation with up to 6.0 Å and more than 2.0 Å can be seen in the proteins' C-terminal tail and loop region, respectively. Compared to these loop regions, most of the helical regions of the predicted aquaporin model can be observed with smaller RMSF values. It indicates lower flexibility of the residues in these regions when simulated at different temperatures. The reason may be due to the hydrogen bond that holds the helical conformation of the proteins resulting in less fluctuation of the residues in the regions (Hub et al., 2009).

However, some of the aquaporin helical structures that lose shape can be observed during the MD simulation. It proves the flexibility of the loop regions that face the extracellular and intracellular side and the loss of some of the aquaporin helical structure when simulated in water at various temperatures. Besides that, as compared in Figure 3, the loop region that connects between H3 and H4 of both predicted aquaporin (Figure 6) shows longer length and predominance with more small residue side chains which can be observed in the most secondary structure of psychrophilic proteins for their higher flexibility in low temperature (Schmidt & Sturgis, 2017).

Channel Radius

Due to the selectivity filter formed by Phe43, His172, Arg187, and Thr181 [Figure 4 (a)] of the aquaporin model, the channel diameter is reduced to be very small, sterically excluding

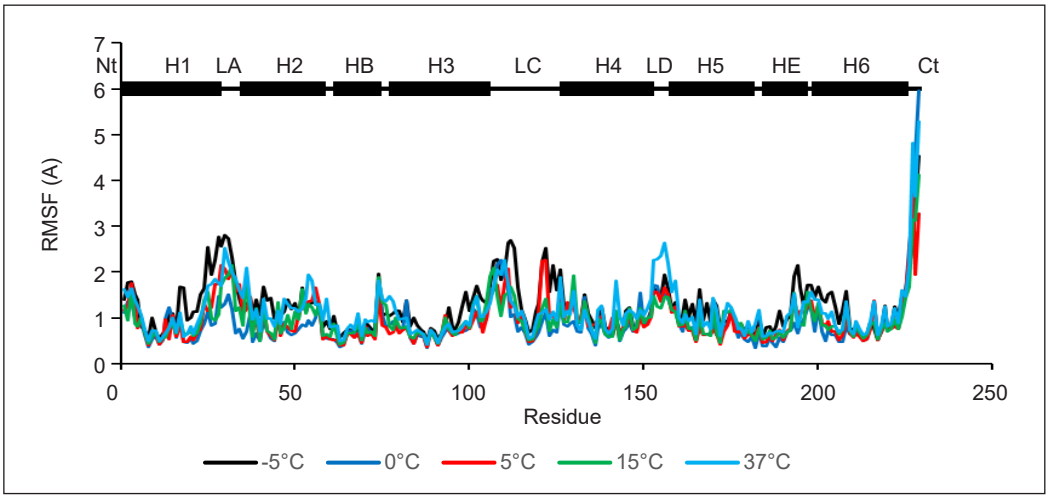

Figure 6. Root Mean Square Fluctuation (RMSF) as functions of time for PaqpZ2_AMS3 atoms. The secondary structure of the proteins was displayed at the top, indicating helices (H1 to H6), half-helices (HB and HE), loops (LA to LD), and termini (Nt and Ct).

the passage of molecules larger than water. This section has the narrowest diameter size in the channel as computed by HOLE 2.0 software (Figure 7) (Brezovsky et al., 2013). In the middle section of the channel, the two conserved Asn-Pro-Ala (NPA) motifs were observed in Asn63 and Asn184 for PAqpZ2_AMS3. The channel radius of each predicted aquaporin monomer was displayed in Figure 7. The program HOLE 2.0 software was used to achieve the pore radius of PAqpZ2_AMS3 monomers along the channel in the z-direction. The pore radius was obtained from configurations of the last frame structure over the 10 ns of the MD simulation. According to Figure 7, the three-dimensional visualization of a monomer pore size was presented as red, which represents the parts that are inaccessible to the water with a pore radius less than 1.15 Å, green for the parts that are accessible to water with a radius between 1.15 Å to 2.30 Å, and blue for the parts that are greater than 2.30 Å (Brezovsky et al. 2013).

The smallest pore radius of PAqpZ2_AMS3 after simulated at -5ºC for 10 ns can be seen above in the aquaporin selectivity filter Figure 7. As predicted by the HOLE 2.0 software, the amino acid residues responsible for the narrowest pore radius calculated were Phe36 and Asp180. It shows that the aquaporin Phe36 and Asp180 residues adopted a conformation that more effectively blocks the channel. Its motion was accompanied by a temperature-driven rearrangement of the water molecules inside the channel. A temperature of -5ºC induced both residues to populate exclusively deeper positions inside the water channel. It proves the flexibility of the residues when simulated in water at different temperatures.

Figure 8 depicts the superposition of the initial and final structures of PAqpZ2_AMS3 simulated at -5ºC after 10 ns. The Cα-RMSD calculated between the Phe36 and Asn180

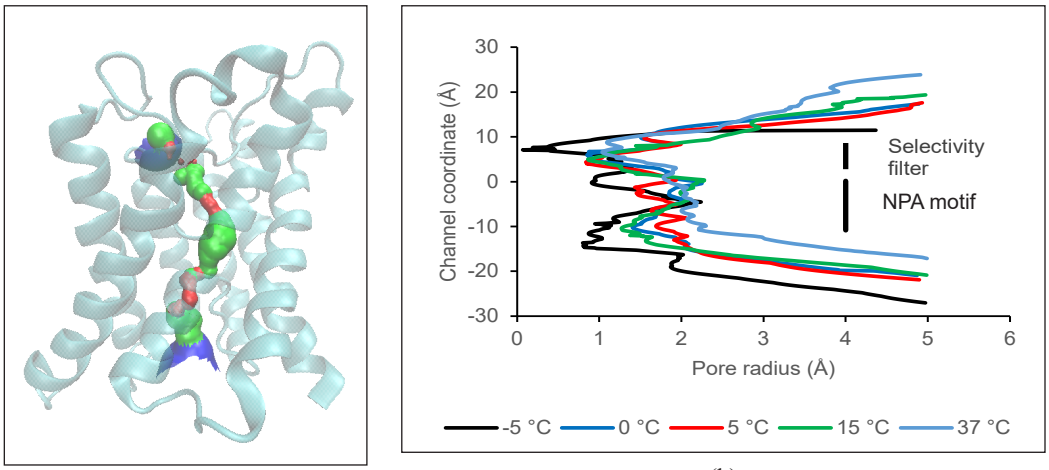

(a) (b)

Figure 7. The pore radius of the final structure. The 10 ns of (a) PAqpZ2_AMS3 model simulated in -5°C visualized with the water pore outline. On the extracellular side of PAqpZ2_AMS3, the channel is blocked. The calculated pore diameter versus the z coordinate of each final structure of PAqpZ2_AMS3 is simulated at various temperatures.

residues in initial and final structures of the PAqpZ2_AMS3 that are involved in blocking the water column is 4.63 Å and 0.75 Å, respectively. Asn180 is the amino acid from the NPA motif, and Phe36 is known to be the water-gating amino acid, thus acting as the selectivity filter in PAqpZ2_AMS3. This result led to the hypothesis that the Phe36 and Asn180 residues of PAqpZ2_AMS3 are more flexible as their conformation is rearranged in low temperatures leading to a decrease of the aquaporin water column and next blocking the channel.

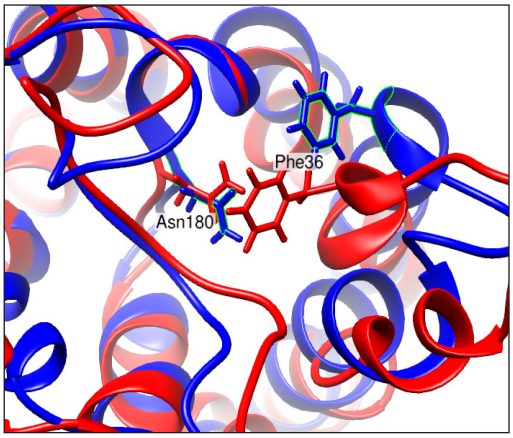

Figure 8. Top view of superposed initial (blue) and final (red) structure of PAqpZ2_AMS3 simulated at -5°C. The Phe36 and Asn180 residues block the water column.

CONCLUSION

This structural and dynamic study of putative aquaporin from Antarctic *Pseudomonas* sp. strain AMS3 provides insights into the mechanistic properties of the water transport protein when simulated in water at various temperatures. The MD simulation results suggest that the aquaporin model can remain stable and flexible throughout the simulation under different temperatures. In addition, the position of Phe36 and Asn180 residues in PAqpZ2_AMS3 were rearranged after 10 ns in -5ºC MD simulation, leading to changes in the aquaporin water column size and next blocking the channel. The information obtained from this identified psychrophilic water channel protein provides new information about this protein's structural adaptability at low temperatures, which may be useful tools for cryogenic industrial applications and molecular engineering.

Future studies will be highly interesting to test this *in silico* analyses and its physiological connection to the channel-blocking mechanism. Furthermore, aquaporin should be simulated in its tetrameric form, and its single-channel water permeability constant should be compared to that of other aquaporin family members. In addition, water orientation inside this protein pore should be studied to provide information and understanding of this psychrophilic aquaporin's cold adaptation and structural insights.

ACKNOWLEDGEMENT

The Ministry of Education supported this project through the Fundamental Research Grant Scheme (FRGS/1/2019/STG04/UPM/02/04).

REFERENCES

Altschul, S. F., Gish, W., Miller, W., Myers, E. W., & Lipman, D. J. (1990). Basic local alignment search tool. *Journal of Molecular Biology, 215*(3), 403-410. https://doi.org/10.1016/S0022-2836(05)80360-2

Aponte-Santamaría, C., Fischer, G., Båth, P., Neutze, R., & de Groot, B. L. (2017). Temperature dependence of protein-water interactions in a gated yeast aquaporin. *Scientific Reports*, *7*(1), 1-14. https://doi.org/10.1038/s41598-017-04180-z

Araya-Secchi, R., Garate, J. A., Holmes, D. S., & Perez-Acle, T. (2011). Molecular dynamics study of the archaeal aquaporin AqpM. *BioMed Central Genomics, 12*(4), 1-13. https://doi.org/10.1186/1471-2164-12-S4-S8

Bienert, S., Waterhouse, A., de Beer, T. A., Tauriello, G., Studer, G., Bordoli, L., & Schwede, T. (2017). The SWISS-MODEL Repository-new features and functionality. *Nucleic Acids Research*, *45*, 313-319. https://doi.org/10.1093/nar/gkw1132

Brezovsky, J., Chovancova, E., Gora, A., Pavelka, A., Biedermannova, L., & Damborsky, J. (2013). Software tools for identification, visualization and analysis of protein tunnels and channels. *Biotechnology Advances*, *31*(1), 38-49. https://doi.org/10.1016/j.biotechadv.2012.02.002

Brown, D. (2017). The discovery of water channels (aquaporins). *Annals of Nutrition and Metabolism*, *70*(1), 37-42. https://doi.org/10.1159/000463061

Cho, C. H., Urquidi, J., Singh, S., Park, S. C., & Robinson, G. W. (2002). Pressure Effect on the density of water. *The Journal of Physical Chemistry A*, *106*(33), 7557-7561. https://doi.org/10.1021/jp0136260

Cohen, E. (2012). Roles of aquaporins in osmoregulation, desiccation and cold hardiness in insects. *Entomology, Ornithology & Herpetology, 1*, 1-17. https://doi.org/10.4172/2161-0983.S1-001

Colovos, C., & Yeates, T. O. (1993). Verification of protein structures: Patterns of nonbonded atomic interactions. *Protein Science*, *2*(9), 1511-1519. https://doi.org/10.1002/pro.5560020916

De Maayer, P., Anderson, D., Cary, C., & Cowan, D. A. (2014). Some like it cold: Understanding the survival strategies of psychrophiles. *European Molecular Biology Organization Reports, 15*(5), 508-517. https://doi.org/10.1002/embr.201338170

Donkor, E. S., Dayie, N. T., & Adiku, T. K. (2014). Bioinformatics with basic local alignment search tool (BLAST) and fast alignment (FASTA). *Journal of Bioinformatics and Sequence Analysis*, *6*(1), 1-6. https://doi.org/10.5897/IJBC2013.0086

Finn, R. N., & Cerda, J. (2015). Evolution and functional diversity of aquaporins. *The Biological Bulletin*, *229*, 6-23. https://doi.org/10.1086/BBLv229n1p6

Gomes, D., Agasse, A., Thiébaud, P., Delrot, S., Gerós, H., & Chaumont, F. (2009). Aquaporins are multifunctional water and solute transporters highly divergent in living organisms. *Biochimica et Biophysica Acta (BBA)-Biomembranes*, *1788*(6), 1213-1228. https://doi.org/10.1016/j.bbamem.2009.03.009

Goto, S. G., Lee Jr, R. E., & Denlinger, D. L. (2015). Aquaporins in the Antarctic midge, an extremophile that relies on dehydration for cold survival. *The Biological Bulletin*, *229*(1), 47-57. https://doi.org/10.1086/BBLv229n1p47

Hedfalk, K., Törnroth-Horsefield, S., Nyblom, M., Johanson, U., Kjellbom, P., & Neutze, R. (2006). Aquaporin gating. *Current Opinion in Structural Biology*, *16*(4), 447-456. https://doi.org/10.1016/j.sbi.2006.06.009

Hospital, A., Goñi, J. R., Orozco, M., & Gelpí, J. L. (2015). Molecular dynamics simulations: Advances and applications. *Advances and Applications in Bioinformatics and Chemistry, 8*, 37-47. https://doi.org/10.2147/AABC.S70333

Hub, J. S., Grubmüller, H., & De Groot, B. L. (2009). Dynamics and energetics of permeation through aquaporins. What do we learn from molecular dynamics simulations.? *Handbook of Experimental Pharmacology, 190,* 57-76. https://doi.org/10.1007/978-3-540-79885-9_3

Kleywegt, G. J. (2000). Validation of protein crystal structures. *Acta Crystallographica Section D: Biological Crystallography*, *56*(3), 249-265. https://doi.org/10.1107/S0907444999016364

Kourghi, M., Nourmohammadi, S., Pei, J. V., Qiu, J., McGaughey, S., Tyerman, S. D., Byrt, C. S., & Yool, A. J. (2017). Divalent cations regulate the ion conductance properties of diverse classes of aquaporins. *International Journal of Molecular Sciences*, *18*(11), Article 2323. https://doi.org/10.3390/ijms18112323

Kozono, D., Ding, X., Iwasaki, I., Meng, X., Kamagata, Y., Agre, P., & Kitagawa, Y. (2003). Functional expression and characterization of an archaeal aquaporin: AqpM from *Methanothermobacter marburgensis*. *Journal of Biological Chemistry*, *278*(12), 10649-10656. https://doi.org/10.1074/jbc.M212418200

Krieger, E., & Vriend, G. (2014). YASARA view - Molecular graphics for all devices from smartphones to workstations. *Bioinformatics*, *30*(20), 2981-2982. https://doi.org/10.1093/bioinformatics/btu426

Lind, U., Järvå, M., Alm Rosenblad, M., Pingitore, P., Karlsson, E., Wrange, A. L., Kamdal, E., Sundell, K., Andre, C., Jonsson, P. R., Havenhand, J., Eriksson, L. A., Hedfalk, K., & Blomberg, A. (2017). Analysis of aquaporins from the euryhaline barnacle *Balanus improvisus* reveals differential expression in response to changes in salinity. *Public Library of Science One, 12*(7), 1-33. https://doi.org/10.1371/journal.pone.0181192

Mannige, R. V., Kundu, J., & Whitelam, S. (2016). The Ramachandran number: An order parameter for protein geometry. *Public Library of Science One, 11*(8), 1-14. https://doi.org/10.1371/journal.pone.0160023

Mathai, J. C., Missner, A., Kügler, P., Saparov, S. M., Zeidel, M. L., Lee, J. K., & Pohl, P. (2009). No facilitator required for membrane transport of hydrogen sulfide. *Proceedings of the National Academy of Sciences*, *106*(39), 16633-16638. https://doi.org/10.1073/pnas.0902952106

Németh-Cahalan, K. L., & Hall, J. E. (2000). pH and calcium regulate the water permeability of aquaporin 0. *The Journal of Biological Chemistry*, *275*(10), 6777-6782. https://doi.org/10.1074/jbc.275.10.6777

Sachdeva, R., & Singh, B. (2014). Insights into structural mechanisms of gating induced regulation of aquaporins. *Progress in Biophysics and Molecular Biology*, *114*(2), 69-79. https://doi.org/10.1016/j.pbiomolbio.2014.01.002

Salomon-Ferrer, R., Case, D. A., & Walker, R. C. (2013). An overview of the Amber biomolecular simulation package. *Wiley Interdisciplinary Reviews: Computational Molecular Science*, *3*(2), 198-210. https://doi.org/10.1002/wcms.1121

Savage, D. F., Egea, P. F., Robles-Colmenares, Y., O'Connell III, J. D., Stroud, R. M., & Simon, S. (2003). Architecture and selectivity in aquaporins: 2.5 Å X-ray structure of aquaporin Z. *Public Library of Science Biology, 1*(3), 334-340. https://doi.org/10.1371/journal.pbio.0000072

Schmidt, V., & Sturgis, J. N. (2017). Making monomeric aquaporin Z by disrupting the hydrophobic tetramer interface. *American Chemical Society Omega, 2,* 3017-3027. https://doi.org/10.1021/acsomega.7b00261

Tong, H., Hu, Q., Zhu, L., & Dong, X. (2019). Prokaryotic aquaporins. *Cells*, *8*(11), Article 1316. https://doi.org/10.3390/cells8111316

Woo, J., Chae, Y. K., Jang, S. J., Kim, M. S., Baek, J. H., Park, J. C., Trink, B., Ratovitski, E., Lee, T., Park, B., Park, M., Kang, J. H., Soria, J. C., Lee, J., Califano, J., Sidransky, D., & Moon, C. (2008). Membrane trafficking of AQP5 and cAMP dependent phosphorylation in bronchial epithelium. *Biochemical and Biophysical Research Communications*, *366*(2), 321-327. https://doi.org/10.1016/j.bbrc.2007.11.078

Zhou, A. Q., O'Hern, C. S., & Regan, L. (2011). Revisiting the Ramachandran plot from a new angle. *Protein Science*, *20*, 1166-1171. https://doi.org/10.1002/pro.644